Design, Behavior, and Recycling of Silica-Supported CuBr−Bipyridine ATRP Catalysts

Joseph V. Nguyen and Christopher W. Jones*

School of Chemical and Biomolecular Engineering, Georgia Institute of Technology, 311 Ferst Drive NW, Atlanta, Georgia 30332

Received September 24, 2003; Revised Manuscript Received December 3, 2003

ABSTRACT: A new strategy for immobilizing CuBr/bipyridine (bpy) complexes on silica surfaces is described. An immobilizable, organosilane-containing bpy ligand (SdMBpyTMS) is synthesized and complexed with CuBr followed by addition to four different silica supports, mesoporous SBA-15 with 50 and 100 Å pores, controlled pore glass (CPG) with 240 Å pores, and nonporous Cab-O-Sil EH5. The resulting solids are characterized by a battery of techniques including thermogravimetric analysis/differential scanning calorimetry (TGA/DSC), FT-Raman spectroscopy, ^{13}C and ^{29}Si magic angle spinning (MAS) and cross-polarization magic angle spinning (CP-MAS) spectroscopy, low-temperature nitrogen physisorption, and elemental analysis. Characterization of these solids revealed that a mixture of covalently immobilized mono- and bis-copper coordinated complexes, uncoordinated ligand, and in some cases physisorbed copper exists on the silica surface. The resulting solids are utilized for ATRP of methyl methacrylate (MMA). Whereas catalysts supported on mesoporous SBA-15 are ineffective at controlling the polymerization, CuBr/SdMBpy complexes immobilized on CPG(240) and Cab-O-Sil are effective at mediating the controlled polymerization of methyl methacrylate. Polymerizations with these catalysts achieved >70% conversion, narrow molecular weight distributions (1.29 < PDI < 1.52), and low (undetectable) residual copper content in the final polymer. Application of the "immobilized/soluble hybrid" methodology with these silica supported catalysts did not result in well-controlled polymerizations due to strong partitioning of the soluble catalyst onto the silica support under the conditions employed here, perhaps elucidating a limitation of this methodology with silica-supported catalysts. A new methodology for catalyst regeneration is described utilizing a simple treatment of the used catalyst with AIBN. The AIBN regenerated catalysts can be recycled with moderate conversions and narrow molecular weight distributions comparable to the first catalyst use.

Introduction

Atom transfer radical polymerization (ATRP) has been a subject of intense research since its discovery in 1995 by Matyjaszewski[1−3] and Sawamoto[4] due to its ability to control polymer architecture (i.e., MW, PDI, and end functionality) and its general applicability to a wide range of monomers and broad experimental conditions.[5] Utilizing a metal/ligand complex with a high affinity toward halogen atoms and two accessible oxidation states separated by one electron, a dynamic equilibrium that is strongly shifted toward deactivation is established ($k_{act} \ll k_{deact}$), keeping the overall radical concentration low and allowing for controlled polymerizations (see Scheme 1). Despite a small amount of bimolecular radical coupling or termination reactions that often occur, well-behaved ATRP, with limited termination, affords polymers with narrow molecular weight distributions (i.e., PDI ∼ 1.2 or better).

A key technical hurdle associated with ATRP is the recovery of the metal complex catalyst from the product polymer. Although many postpolymerization purification workup methods have been devised to remove the soluble catalyst from the polymer,[6−12] a solid, recoverable, and recyclable catalyst is the most attractive solution. There are many examples in the literature involving the immobilization of an ATRP metal/ligand complex on various supports. Matyjaszewski,[13−17] Haddleton,[18,19] Brittain,[20,21] Zhu,[22−28] and others[29−31] have reported covalently immobilized ATRP catalysts. However, because of a variety of factors, these surface-mediated polymerizations often allow for only limited control over the polymerization.

Scheme 1

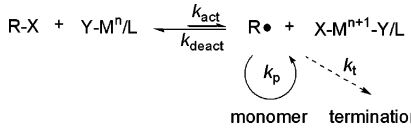

A number of factors can contribute to the efficacy of supported ATRP catalysts in controlling the course of radical polymerizations. The primary issue appears to concern accessibility of the metal complexes to the growing polymer chains. Poor polymerization control in earlier investigations was generally attributed to a poor deactivation of the growing polymer chain,[13,15] as shown in Scheme 2a−d. Once the initiator is activated (Scheme 2b), propagation of monomer at the growing radical is uncontrolled (Scheme 2c) because the deactivation step is affected by the mobility and accessibility of the immobilized catalyst on the support and the rate of diffusion of the polymer chains in the reaction mixture (Scheme 2d). If the growing radical chain does not encounter a high oxidation state metal complex and become deactivated readily enough, propagation of the polymer chain becomes uncontrolled. For this reason, catalysts that have highly accessible complexes such as those that use flexible/soluble supports[20,21,24,27] or long surface−complex linkages[26] are among the most effective. Hence, the size, porosity, and solubility of the catalyst particle ultimately affect the polymerization. Most recently, Matyjaszewski[14,15] introduced a mixed heterogeneous/homogeneous catalyst system ("immobi-

* To whom correspondence should be addressed. E-mail cjones@chbe.gatech.edu.

10.1021/ma0354391 CCC: $27.50
Published on Web 01/22/2004

Scheme 2

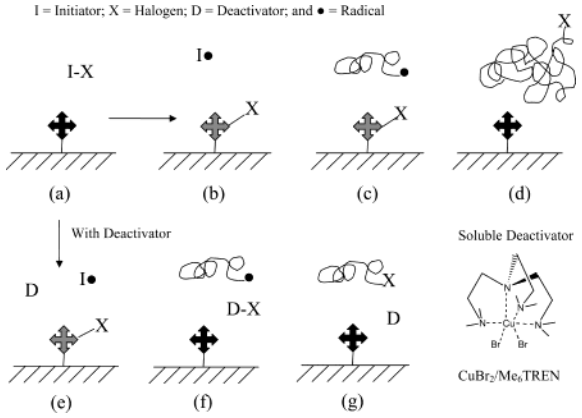

lized/soluble hybrid system") to gain better control over the polymerization. It was found that by adding a small amount of soluble deactivator complex, $CuBr_2$/Me_6TREN, the deactivation process was facilitated, and the polymerization proceeded in a controlled manner, as shown in Scheme 2e−g. The soluble deactivator is proposed to act as a "shuttling agent", transferring the halogen to the growing polymer chain, thus deactivating the chain and keeping the overall radical concentration low (Scheme 2f,g). Even though only a small percentage of soluble deactivator is introduced into the polymerization, soluble copper catalyst is eventually left in the polymer product. Although the clever use of this soluble deactivator appears to be among the best solutions proposed to date for giving a (mostly) recoverable catalyst with good control, based on current literature reports, it may still be feasible that alternate solid catalyst designs could yield a well-behaved catalyst that is entirely heterogeneous and inexpensive. In particular, little attention has been paid to the diversity of different metal complex structures that can occur in the supported catalysts and the potential varying reactivities of these immobilized species. In fact, most immobilized ATRP catalysts are prepared using a multistep grafting methodology that has been shown to result in multisited solid materials.[30]

Here, we report the synthesis of a well-defined, immobilizable bpy ligand, 4-{4-[3-(trimethyoxysilanyl)propylsulfanyl]butyl}-4′-methyl-2,2′-bipyridyl or SdMBpyTMS (Scheme 3), and the direct immobilization of CuBr/SdMBpyTMS ATRP complexes on several silica supports of varying structure and porosity. The new catalysts are evaluated in the ATRP of methyl methacrylate (MMA) with a focus on polymerization control, catalyst recovery/leaching, and catalyst recycle.

Experimental Section

Chemicals. Chloroform-*d* ($CDCl_3$, Cambridge Isotope Laboratories, Inc.; 99.8%), allyl bromide (Aldrich; 99%), diisopropylamine (DiPA; Acros; 99+%), 1-propanethiol (Acros; 98%), dipropyl sulfide (DPS; Acros; 98+%), and 2-bromoproprionitrile (BPN; Aldrich; 97%) were dried over 4 Å molecular sieves and stored under dry nitrogen. (3-Mercaptopropyl)trimethoxysilane (MPTMS; Aldrich; 95%) and copper(II) bromide ($CuBr_2$; Aldrich; 99%) were used as received and stored under dry nitrogen. *n*-Butyllithium (*n*-BuLi; Aldrich; 0.6 M in hexanes), poly(ethylene glycol)-*block*-poly(propylene glycol)-*block*-poly(ethylene glycol) (EO−PO−EO; Aldrich), hydrochloric acid (HCl; JT-Baker; A.C.S. Reagent), tetraethyl orthosilicate (TEOS; Acros; 98%), hexamethyldisilazane (HMDS; Adlrich; 99%), and 1,3,5-trimethylbenzene (TMB; Aldrich; 97%) were used as received. Copper(I) bromide (CuBr; Acros; 98%) was purified by stirring in glacial acetic acid for 5 h, washed with absolute ethanol and anhydrous diethyl ether, dried under vacuum for 12 h at room temperature, and stored under dry nitrogen. 4,4′-Dimethyl-2,2′-dipyridyl (dMBpy; Aldrich; 99%) and 2,2′-azobis(2-methylpropionitrile) (AIBN; Aldrich; 99%) were recrystallized in methanol, recovered, dried under vacuum at room temperature for 12 h, and stored under dry nitrogen. Methyl methacrylate (MMA; Aldrich; 99%) was passed three times through an inhibitor removal column (Aldrich-311332), distilled once under reduced pressure, degassed by three freeze/thaw cycles, and stored under nitrogen at −22 °C. Toluene for polymerization (Acros; 99.8%) was distilled under reduced pressure over sodium/benzophenone, degassed by three freeze/thaw cycles, and stored under nitrogen. 2-Bromopropionitrile was stored in a 0.47 M stock solution in dry toluene under nitrogen. THF (Aldrich, HPLC grade inhibitor-free, >99%) was used as received for the eluent in GPC analysis. Cab-O-Sil EH5 (Cabot) and CPG (CPG(240); CPG, Inc.; CPG00240B) were dried under vacuum for 12 h at room temperature and stored under nitrogen. Hexanes (Aldrich; >99%), methylene chloride (CH_2Cl_2; Aldrich; >99%), tetrahydrofuran (THF; Aldrich; >99%), and diethyl ether (Aldrich; >99%) were dried and deoxygenated using a purification system and stored under nitrogen in a glovebox.[32] Tris(2-(dimethylamino)ethyl)amine (Me_6TREN) was synthesized according to literature procedures,[33] dried with $MgSO_4$, and stored under nitrogen in a glovebox.

Preparation of SBA-15 (50 and 100 Å Pores). Mesoporous silica SBA-15 was synthesized utilizing the triblock poly(ethylene oxide)−poly(propylene oxide)−poly(ethylene oxide) (EO−PO−EO) nonionic surfactant as the structure-directing agent.[34,35] In a typical preparation, 12.43 g of EO−PO−EO, 273.92 g of DI H_2O, and 86.60 g of 38% aqueous HCl were stirred at room temperature until the triblock copolymer completely dissolved. Then 27.05 g of TEOS was added to the solution and stirred for 5 min. The mixture was distributed into 10 Parr Teflon-line autoclaves and agitated at 50 °C for 20 h. The solid product was recovered by filtration, washed with DI H_2O extensively, and air-dried at 50 °C overnight. Calcination was carried out by slowly increasing temperature from room temperature to 200 °C at 1.2 K/min under a nitrogen-enriched atmosphere. The temperature was held at 200 °C for 1 h and then slowly increased to 500 °C at 2 K/min under oxygen-enriched atmosphere. The temperature was held at 500 °C for 6 h. The solid product was dried under vacuum for 12 h and stored under dry nitrogen in a glovebox, yielding approximately 8 g of solid.

Scheme 3

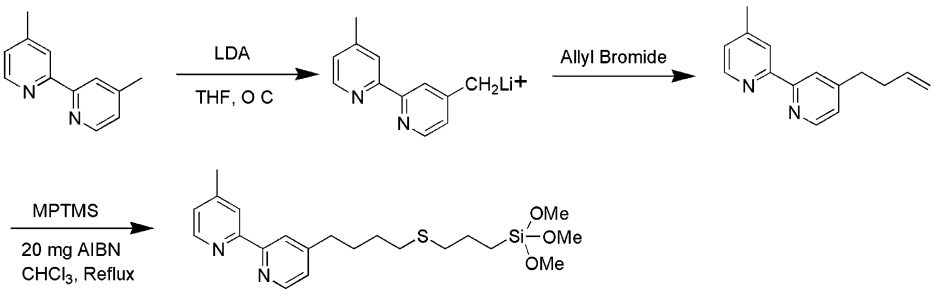

Table 1. Elemental Analysis Results for Silica-Supported CuBr/SdMBpy Catalysts

entry	catalysts	% C	% H	% N	% Si	% Cu
1	SBA15(50)-CuBr/SdMBpy	16.28	1.99	1.64	28.70	2.55
2	SBA15(100)-CuBr/SdMBpy	15.67	2.55	2.54	29.32	3.97
3	CPG(240)-CuBr/SdMBpy	7.13	1.51	1.80	32.25	2.44
4	Cab-O-Sil-CuBr/SdMBpy	13.93	1.34	1.64	34.49	2.39

Large pore SBA-15(100) was synthesized similar to the 50 Å material except 1,3,5-trimethylbenzene (TMB) was used as a swelling cosolvent. In a typical preparation, 12.00 g of EO−PO−EO, 317.77 g of DI H_2O, 1.50 g of TMB, and 86.60 g of 38% aqueous HCl were stirred at room temperature until the triblock copolymer completely dissolved. Then 25.63 g of TEOS was added to the solution and stirred for 5 min. The mixture was distributed into 10 Parr Teflon-line autoclaves and agitated at 35 °C for 20 h and then aged at 100 °C without stirring for 24 h. The solid product was recovered by filtration, washed with DI H_2O extensively, and air-dried at 50 °C overnight. Calcination was carried out under the same conditions described for the 50 Å pore material. The solid product was dried under vacuum for 12 h and stored under dry nitrogen in a glovebox, yielding approximately 7 g of solid.

Syntheses. All syntheses described below were carried out under dry nitrogen in a glovebox unless otherwise noted. Schlenk techniques were used for manipulating reaction mixtures outside the nitrogen glovebox. All solvents used in the synthesis of these materials were anhydrous and deoxygenated.

Preparation of 4′-But-3-enyl-4-methyl-2,2′-bipyridinyl (Allyl dMBpy). Preparation was performed as previously described.[36] Dry THF (50 mL) and 1.449 g of DiPA (0.0142 mol) were added to a 250 mL flask in a nitrogen glovebox. The reaction mixture was cooled to 0 °C, and 8.4 mL of *n*-BuLi (0.0132 mol) was slowly added dropwise under positive argon pressure. After the addition was complete, the reaction mixture was stirred at 0 °C for 30 min followed by addition of a solution of 2.422 g of dMBpy (0.0132 mol) in dry THF (100 mL) by cannula. The reaction mixture immediately turned a dark purplish color and was allowed to stir at 0 °C for an additional 1 h under argon on a Schlenk line. Subsequently, a mixture of dry THF (10 mL) and 1.620 g of allyl bromide (0.0132 mol) were added dropwise by syringe under positive argon pressure. The reaction mixture was stirred at 0 °C for an additional 2 h, and then it was allowed to warm to room temperature overnight. The reaction mixture was subsequently quenched with 10 mL of DI H_2O, and the THF was removed by rotovap. The resulting product was extracted with diethyl ether and dried over $MgSO_4$. The final product was recovered by rotovap to yield 2.4 g of viscous orange oil. The product was purified by vacuum sublimation at 100 °C to remove unsubstituted dMBpy. The product was degassed and stored under dry nitrogen in a glovebox. $C_{15}H_{16}N_2$ (2.81 g, yield 95%) ^{1}H NMR ($CDCl_3$): $\delta = 2.43$ (s, 3H, $-CH_3$), $\delta = 2.46$ (m, 2H, $-CH_2CH_2$-$CH{=}CH_2$), $\delta = 2.80$ (t, 2H, $-CH_2CH_2CH{=}CH_2$), $\delta = 5.02$ (t, 2H, $-CH_2CH_2CH{=}CH_2$), $\delta = 5.84$ (m, 1H, $-CH_2CH_2CH =$ CH_2), $\delta = 7.13$ (d, 2H, $-$(CH$_3$ or CH$_2$)$-$CCHCHNCCH$-$), $\delta =$ 8.24 (s, 2H, $-$(CH$_3$ or CH$_2$)$-$CCHCHNCC*H*-), $\delta = 8.54$ (d, 2H, $-$(CH$_3$ or CH$_2$)$-$CCHC*H*NCCH$-$).

Preparation of 4′-{4-[3-(Trimethoxysilanyl)propylsulfanyl]butyl}-4-methyl-2,2′-bipyridinyl (SdMBpyTMS). A mixture of 2.0 g of Allyl dMBpy (8.90 mmol), 8.75 g of MPTMS (44.5 mmol), 20 mg of AIBN, and dry $CHCl_3$ (50 mL) were added to a 100 mL flask. The reaction mixture was refluxed for 12 h under argon. The $CHCl_3$ was removed by vacuum, and the product was isolated by a careful vacuum distillation of the light volatiles and excess MPTMS at 80 °C for 1 h at 10 mTorr to yield 3.75 g of a viscous orange oil. The product was degassed and stored under dry nitrogen in a glovebox. $C_{21}H_{32}N_2O_3SSi$ (3.70 g, yield 99%). ^{1}H NMR ($CDCl_3$): $\delta = 0.77$ (d, 2H, $-CH_2CH_2Si-$), $\delta = 1.66$ (m, 4H, $-CH_2CH_2SCH_2CH_2-$), $\delta = 1.80$ (m, 2H, $-CH_2CH_2CH_2SCH_2CH_2CH_2Si-$), $\delta = 2.43$ (s, 3H, $-CH_3$), $\delta = 2.50$ (m, 4H, $-CH_2SCH_2-$), $\delta = 2.71$ (t, 2H, $-CH_2CH_2CH_2CH_2SCH_2CH_2CH_2Si-$), $\delta = 3.55$ (s, 9H, $-Si(OCH_3)_3$), $\delta = 7.12$ (d, 2H, $-$(CH$_3$ or CH$_2$)$-$CCHCHNCCH$-$), $\delta = 8.22$ (s, 2H, $-$(CH$_3$ or CH$_2$)$-$CCHCHNCC*H*-), $\delta = 8.54$ (d, 2H, $-$(CH$_3$ or CH$_2$)$-$CCHC*H*NCCH$-$).

Preparation of 4-Methyl-4′-(4-propylsulfanylbutyl)-2,2′-bipyridinyl (pSdMBpy). A mixture of 2.0 g of Allyl dMBpy (8.90 mmol), 3.40 g of 1-propanethiol (44.5 mmol), 20 mg of AIBN, and dry $CHCl_3$ (50 mL) were added to a 100 mL flask. The reaction mixture was refluxed for 12 h under argon. The $CHCl_3$ was removed by vacuum, and the product was isolated by a careful vacuum distillation of the light volatiles and excess 1-propanethiol at 80 °C for 1 h at 10 mTorr to yield 3.75 g of a viscous orange oil. $C_{18}H_{24}N_2S$ (2.67 g, yield >99%). ^{1}H NMR ($CDCl_3$): $\delta = 0.95$ (t, 3H, $-SCH_2CH_2CH_3$), $\delta = 1.58$ (m, 4H, $-CH_2CH_2SCH_2CH_2-$), $\delta = 1.79$ (m, 2H, $-CH_2CH_2$-$CH_2SCH_2CH_2CH_3$), $\delta = 2.42$ (s, 3H, $-CH_3$), $\delta = 2.49$ (m, 4H, $-CH_2SCH_2-$), $\delta = 2.70$ (t, 2H, $-CH_2CH_2CH_2CH_2SCH_2CH_2$-$CH_3$), $\delta = 7.13$ (d, 2H, $-$(CH$_3$ or CH$_2$)$-$CCHCHNCCH$-$), $\delta =$ 8.21 (s, 2H, $-$(CH$_3$ or CH$_2$)$-$CCHCHNCC*H*$-$), $\delta = 8.55$ (d, 2H, $-$(CH$_3$ or CH$_2$)$-$CCHC*H*NCCH$-$).

Preparation of SBA-15(50 Å)-CuBr/SdMBpy Immobilized Catalyst. To a 100 mL bottom flask, a solution of 1.00 g of SdMBpyTMS (2.37 mmol) and 5 mL of dry toluene was slowly added to a stirring mixture of 0.17 g of CuBr (1.86 mmol) in 50 mL of dry toluene at 70 °C in a nitrogen glovebox. The resulting light brown mixture was then stirred at 70 °C for 30 min under nitrogen or until the reaction mixture appears to be a dark reddish homogeneous solution. Then 2.00 g of SBA-15 (50 Å pores) was added to the reaction mixture, sealed with a valve, and removed from the nitrogen glovebox. Then the reaction mixture was stirred at 110 °C for 48 h under argon. The reaction flask was transferred into the nitrogen glovebox, and the solid product was recovered and washed, once with 100 mL of dry toluene, once with 100 mL of dry hexanes, and once with copious amount of dry dichloromethane until the solvent filtered out was clear. The dark reddish powder was dried under vacuum at room temperature for 12 h and stored under dry nitrogen in a glovebox. CHN, Si, and Cu analyses are summarized in Table 1.

Preparation of SBA-15(100 Å), CPG(240 Å), and Cab-O-Sil EH5−CuBr/SdMBpy Immobilized Catalysts. In a manner similar to the procedure described above for SBA-15 (50 Å pores), a supported CuBr/SdMBpy complex was immobilized on a larger pore SBA-15 (100 Å pores), CPG (240 Å pores), and nonporous Cab-O-Sil EH5 silica supports. All the immobilized catalysts were recovered, washed, and stored under the same conditions. CHN, Si, and Cu analyses are summarized in Table 1.

Polymerization. For polymerization with the homogeneous CuBr/dMBpy or CuBr/pSdMBpy catalyst, the following recipe was typical: [MMA]/[dMBpy]/[Cu]/[BPN] = *X*/2/1/1 in *Y*% by v/v MMA in toluene or diphenyl ether ($X = 300$, $Y = 50$ or $X = 100$, $Y = 25$). For example, ($X = 300$, $Y = 50$ in toluene) to a 50 mL round-bottom flask with a sidearm valve, 4.00 g of MMA (0.040 mol, 4.24 mL), 0.049 g of dMBpy (0.266 mmol), 0.019 g of CuBr (0.133 mmol), and 0.06 g of BPN (0.133 mmol, 283 μL of initiator stock solution) were added in 3.68 g of toluene (4.24 mL) under nitrogen. The polymerization vessel was immersed in an oil bath preset to 90 °C. At set time intervals, 0.1 mL aliquots of polymerization solution were removed via syringe and placed in a vial. The vials were immediately quenched in a dry ice/acetone bath. Subsequently, 25 μL of sample was added to 1.5 mL of THF for GC conversion analysis. The remaining sample was dried, redissolved in HPLC grade THF to 8.0 mg/mL, and filtered through a Gelman Acrodisc PTFE filter (0.2 μm) for GPC analysis. The conversion of MMA was followed by GC, and molecular weights and molecular weight distributions were determined by GPC.

For polymerization using immobilized silica-CuBr/SdMBpy catalysts, the following recipe was typical: [MMA]/[Cu]/[BPN] = *X*/1/1 in *Y*% by v/v MMA in toluene at 90 °C (*X* = 300, *Y* = 50 or *X* = 100, *Y* = 25). For instance, (*X* = 100, *Y* = 25) to a 10 mL Schlenk tube with a sidearm valve, 0.20 g of CPG(240)-CuBr/SdMBpy (8.82×10^{-2} mmol of Cu, 0.44 mmol Cu/g of catalyst), 0.80 g of MMA (8.82 mmol), and 170 μL of initiator stock solution BPN (8.82×10^{-2} mmol) were added to 2.19 g of toluene under nitrogen. The polymerization vessel was immersed in an oil bath preset to 90 °C. Samples were taken at preset times and quenched using the procedure described above. Kinetic analysis and polymer characterization were carried out in a similar manner described for the homogeneous polymerization. After the polymerization, the catalysts were recovered from the remaining polymerization solution by sedimentation (SBA15(50 and 100)) and CPG(240)) or centrifugation (Cab-O-Sil EH5). The polymers were then precipitated in 50 mL of hexane, and the polymers were recovered and dried as a white powder. The dried polymers were analyzed for trace amounts of copper.

Catalyst Regeneration. The immobilized silica−CuBr/SdMBpy catalysts were regenerated with AIBN after each use when catalyst recycling was planned. The used catalysts were recovered from the polymerization solution by filtration or centrifugation and washed with copious amounts of toluene. The catalyst was transferred into a pressure tube reactor (i.e., 0.20 g of CPG(240)−CuBr/SdMBpy, 0.088 mmol of Cu). Then 3.00 g of toluene and an equivalent of AIBN to Cu (8.82×10^{-2} mmol or 14.45 mg of AIBN) were added to the reaction tube. The pressure tube reactor was sealed and placed in preheated oil bath at 90 °C. The mixture was stirred for 15 min. The pressure tube reactor was transferred into the glovebox where the catalyst was recovered by filtration or centrifugation and washed with copious amounts of toluene and dichloromethane. The catalyst was dried under high vacuum for 12 h and stored under dry nitrogen in a glovebox for further use. Subsequent catalyst regenerations (i.e., second and third regeneration of the same catalyst) were performed in a similar manner described above.

Catalyst Recycling. For polymerization with the immobilized silica−CuBr/SdMBpy catalyst when catalyst recycling was planned, the following recipe was typical: [MMA]/[Cu]/[BPN] = *X*/1/1 in *Y*% by v/v MMA in toluene (*X* = 300, *Y* = 50 or *X* = 100, *Y* = 25). For instance, (*X* = 100, *Y* = 25) to a 10 mL Schlenk tube with a sidearm valve, 0.20 g of regenerated CPG(240)−CuBr/SdMBpy (8.82×10^{-2} mmol of Cu, 0.44 mmol Cu/g of catalyst), 0.80 g of MMA (8.82 mmol), and 170 μL of initiator stock solution BPN (8.82×10^{-2} mmol) were added to 2.19 g of toluene under nitrogen. A 25 μL sample was taken immediately after mixing and prior to start of the polymerization to establish the reference conversion point at time zero. The polymerization vessel was immersed in an oil bath preset to 90 °C for a set time. The polymerization vessel was cooled by immersing in a dry ice/acetone bath and retransferred into a glovebox. A 25 μL sample was taken after the polymerization to determine the final conversion by GC. The polymerization solution was transferred into a 20 mL scintillation vial and filled with toluene (under nitrogen) for catalyst recovery. The vial was then centrifuged for 10 min at 3000 rpm. After centrifugation, the vial containing a lower solid catalysts layer and an upper liquid polymerization solution layer was transferred back into the glovebox, and the supernatant toluene/polymerization solution was decanted. The polymers (first use, second use, etc.) were precipitated from the supernatant toluene/polymer solution described above by addition to 50 mL of hexane. The polymer was recovered and dried. The polymer molecular weight and polydispersity were determined by GPC. If catalyst recycling was planned for subsequent reuse, the procedure described above for catalysts regeneration was performed.

Characterization. Thermogravimetric analysis (TGA) was carried out using a Netzsch simultaneous thermal analyzer STA 409 PC Luxx (TGA/DSC) by heating to 1000 °C at 20 K/min in air. Silica pore diameters and surface areas were determined using nitrogen physisorption data obtained with a Micromeritics ASAP 2000 system. The samples were pretreated at 90 °C for 1 h and 150 °C overnight under vacuum. The surface areas were analyzed by the BET method, and the pore size distribution was determined using the BJH method applied to the adsorption branch of the isotherm.[37] X-ray powder diffraction patterns were recorded using Cu Kα radiation on a Scintag X1 powder diffractometer. FT-Raman spectroscopy was performed using a Bruker IFS 66v/S equipped with dual FT-IR and FT-Raman benches and a CaF_2 beam splitter. ^{1}H and ^{13}C solution NMR measurements were performed using a Mercury Vx 300 MHz with $CDCl_3$ used as solvent. Solid-state ^{13}C and ^{29}Si cross-polarization magic angle spinning (CP-MAS) NMR spectra were collected on a Bruker DSX 300 and 400 MHz instruments, respectively. Typical ^{13}C CP-MAS parameters were 10000 scans, a 90° pulse length of 4 μs, and a delay of 4 s between scans. Typical ^{29}Si CP-MAS parameters were 2000 scans, a 90° pulse length of 5 μs, and a delay of 10 s between scans. Copper and silicon elemental analyses were performed by Galbraith Laboratories, Inc., Knoxville, TN, or Chemisar Laboratories, Guelph, Canada, using ICP-AES. Carbon, hydrogen, and nitrogen contents were determined via CHN analysis by Galbraith Laboratories, Inc., Knoxville, TN, or Chemisar Laboratories, Guelph, Canada. Conversion of the monomer was determined using a Shimadzu GC 14-A gas chromatograph equipped with a FID detector using a HP-5 column (30 m length, 0.25 mm i.d., and 0.25 μm film thickness). The temperature program was heating from 50 to 140 °C at 30 K/min and from 140 to 300 °C at 40 K/min under constant pressure with inlet and detector temperatures set constant at 330 °C. The molecular weight and molecular weight distributions were determined by gel permeation chromatography (GPC) using American Polymer Standards columns (10^5, 10^3, 10^2 Å) equipped with a Waters 510 pump and a Waters 410 differential refractometer. THF was used as an eluent at the flow rate of 1 mL/min. Nine linear PMMA standards (700−2100K) were used for calibration of methyl methacrylate polymers.

Results and Discussion

Synthesis of Immobilizable Bipyridine Ligand. Matyjaszewski,[14,15] Zhu,[24−27] Brittain,[20,21] and Haddleton[18] have all reported useful methods for covalent immobilization of ATRP complexes on polymeric or silica supports. In many cases, excellent control of the polymerization can be obtained.[14,15,20,21,24,26,27] However, in all cases, a multistep grafting procedure was used and this synthetic methodology can lead to heterogeneous materials with a variety of different types of surface species.[30,31] For bpy ligands/complexes covalently tethered on supports, only a multistep grafting method has been reported.[14,38−43] Additional methods of incorporating bpy complexes onto substrates include physical adsorption,[44] ion exchange,[45] encapsulation,[46] and other techniques.[47−52] These ill-defined approaches can also produce materials with many different surface species possessing different activities. Preparation of an immobilizable, preformed CuBr/Bpy complex may allow for the preparation of more well-defined solid materials for supported ATRP. To this end, an immobilizable bpy ligand was synthesized homogeneously using a modified procedure similar to the approach used for supported 4,4′-dimethyl-2,2′-bipyridine (dMBpy) ligands[14,38−40,47] (Scheme 3). A dMBpy precursor was functionalized with an allyl group on one of the molecule's two methyl groups.[36] The terminal double bond gives a versatile handle to synthesize a variety of immobilizable dMBpy ligands. Initial attempts to hydrosilylate the allyl dMBpy with trimethoxysilane in the presence of Pt catalysts failed to produce the desired immobilizable dMBpy ligand, possibly due to coordination of the Pt catalyst by the bpy ligands. To circumvent this problem,

Table 2. Thermogravimetric and Elemental Analysis for Silica-Supported CuBr/SdMBpy Catalysts

entry	catalysts	L loading[a] (mmol/g of cat)	L loading[b] (mmol/g of cat)	Cu loading[c] (mmol/g of cat)	% loaded[d] (TGA, EA)
1	SBA15(50)-CuBr/SdMBpy	0.64	0.66	0.45	141, 137
2	SBA15(100)-CuBr/SdMBpy	0.73	0.73	0.66	182, 182
3	CPG(240)-CuBr/SdMBpy	0.31	0.36	0.44	284, 246
4	Cab-O-Sil-CuBr/SdMBpy	0.58	0.62	0.38	131, 123

[a] Based on thermogravimetric analysis. [b] Based on total carbon content by CHN elemental analysis. [c] Based on total copper content by ICP-AES elemental analysis. [d] Calculated assuming a ligand/metal mole ratio of 2.

Scheme 4

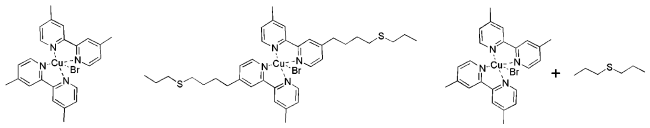

a simple thiol coupling reaction was utilized to make a thioether linkage.[53] Five equivalents of (3-mercaptopropyl)trimethoxysilane (MPTMS) were added to an equivalent of allyl dMBpy in the presence of a catalytic amount of AIBN to produce 4′-{4-[3-(trimethoxysilanyl)propylsulfanyl]-butyl}-4-methyl-2,2′-bipyridinyl or SdMBpyTMS (Scheme 3). The coupling reaction proceeded quantitatively, and by ^{1}H NMR, the concomitant absence of the double bond and thiol protons and the appearance of methylene protons adjacent to the thioether linkage were noted. The SdMBpyTMS compound possesses several important features that make it a good immobilizeable ATRP ligand—a reactive, immobilizable unit, flexible linker, and metal binding sites. It is noted that there are reported syntheses of asymmetric immobilizable bpy organosilanes in the literature; however these materials were never isolated as pure compounds.[40,47] For this work, a homogeneous analogue to SdMBpyTMS was synthesized in a similar manner except without the immobilizable unit (pSdMBpy). This homogeneous analogue will be used to study the effects the sulfur linkage modification may have on the polymerization (Scheme 4b).

Silica Supports. The SBA-15 materials were prepared according to the procedure previously described by Stucky et al.[34,35] For the 100 Å pore material, TMB was used as a swelling agent to increase the pore size. The mesoporous silicates were characterized by nitrogen physisorption to determine the surface area and pore size of the pristine silica supports. The surface areas were 795 and 895 m^2/g for SBA-15(50) and SBA-15(100), respectively. Thermogravimetric analysis approximated the total silanol concentration to be 2.0 mmol of OH/g of solid for 50 and 100 Å materials. X-ray powder diffraction was used to determine the order of the porosity and the overall structure of the SBA-15. The XRD patterns (not shown) were consistent with a hexagonal pore structure.[34,35,37] CPG(240) and Cab-O-Sil EH5 are commercially available silica from CPG, Inc., and Cabot, respectively. The CPG(240) has a particle size of 74−125 μm, a mean pore diameter of 242 Å, a surface area of 88 m^2/g, and 1.05 mmol of OH/g of solid. Cab-O-Sil is a fumed, nonporous silica with multiparticle aggregates having a length of 0.2−0.3 μm (individual particles have nanosized features), a surface area of 335 m^2/g, and 2.7 mmol of OH/g of solid.These silica supports provide a wide range of pore sizes and surface structures to probe how the silica support structure affects the polymerization performance.

Immobilization of CuBr/SdMBpyTMS Complex on Various Silica Supports. The covalent immobilization of CuBr/SdMBpyTMS complex was performed similarly to the "preassembled complex approach" reported previously for immobilized CuBr/PMITMS catalysts (method 4 in ref 30). This approach appeared to result in a more structurally homogeneous immobilized ATRP complex that can allow for polymerization with relatively good control and high conversion using immobilized silica−CuBr/PMI (pyridylmethanimine) catalysts.[30,31] In a nitrogen glovebox, the complex was preassembled (1:2 CuBr/SdMBpyTMS molar ratio, target bis-coordination) in dry toluene at 70 °C before the bare, pristine silica support was added. The reaction mixture was allowed to reflux for 2 days under argon before the immobilized complex was recovered by filtration or centrifugation under nitrogen. An extensive wash with dry dichloromethane was performed to remove excess unreacted ligand or complex and uncoordinated CuBr.[30,31]

The CuBr/SdMBpyTMS complex was covalently immobilized on the following silica supports: SBA-15 (50 and 100 Å pores), CPG (240 Å pores), and nonporous fume silica Cab-O-Sil EH5 (designated as silica support−CuBr/SdMBpy). The compositions of the immobilized catalysts were determined by elemental and thermogravimetric analyses (Tables 1 and 2). The SdMBpy ligand loadings were calculated on the basis of average 1−2 −OMe units reacting with the surface silanols, as determined by ^{29}Si MAS and CP-MAS NMR[54] (spectra not shown). The calculated loadings from TGA and elemental analysis were in good agreement. The ligand and copper loadings were substantially lower than those reported by Matyjaszewski on polymeric supports[14,15] (CuBr/PS8-dMBpy; 2.40 mmol of ligand/g of catalyst and 1.58 mmol of Cu/g of catalyst, respectively). The copper loadings are tabulated using "% loaded" values as previously described:[31]

$$\%\ \text{SdMBpy complexed} = [(\text{mmol of Cu/g of catalyst})/[(\text{mmol of SdMBpy ligand/g of catalyst}^{-1})/2]] \times 100$$

A value of 100% SdMBpy coordinated signifies that the number of Cu atoms is consistent with coordination to two immobilized SdMBpy ligands. Deviations from a 100% mean that uncoordinated SdMBpy ligands must exist (<100%), mono-Cu-coordinated SdMBpy ligands likely exist (100 > X > 200%), or Cu adsorbed to the silica surface with no organic ligand likely exists (>200%). This quantity is an only a measure of the metallation efficiency and should not be used as the only indication of what surface species exist on the silica surface.

The % loaded results suggest that mono- and bis-copper coordinated centers exist on the surface for SBA-15(50 and 100 Å) and Cab-O-Sil supports because the % loaded[31] values were above 100% (Table 2). The copper loading for the CPG(240) immobilized catalyst

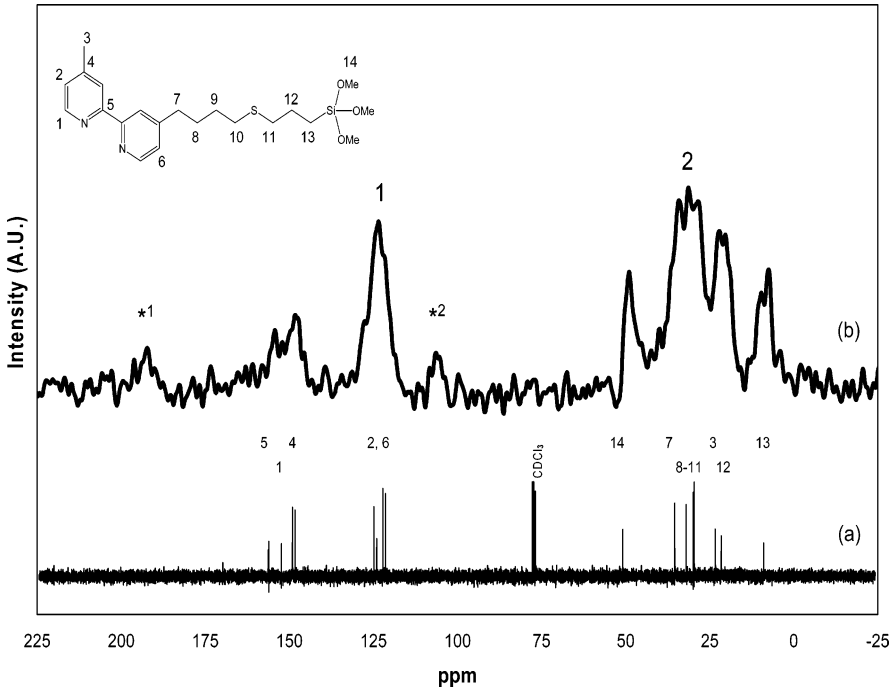

Figure 1. ^{13}C solution and solid-state NMR spectra of (a) SdMBpyTMS and (b) SBA15(100)-SdMBpy by CP-MAS. *X denotes a spinning sideband of signal X.

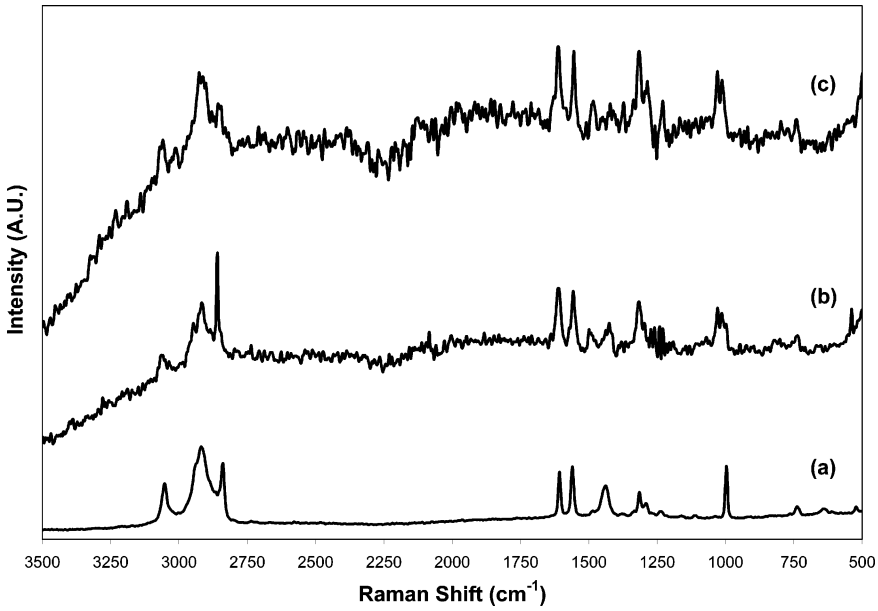

Figure 2. FT-Raman spectra of (a) SdMBpyTMS, (b) SBA15(50)-CuBr/SdMBpy, and (c) SBA15(100)-CuBr/SdMBpy.

suggests that the surface is composed of copper centers coordinated with one SdMBpy ligand, with a fraction of the copper centers physisorbed to the silica surface (% loaded > 200%). Experimental evidence to support these suppositions is given below.

The immobilization of the SdMBpyTMS ligand and complex were characterized by ^{13}C CP-MAS NMR and FT-Raman spectroscopy. The uncoordinated SdMBpyTMS ligand was directly immobilized on to SBA15(100) and probed by ^{13}C CP-MAS NMR spectroscopy (Figure 1). The bottom spectra is the solution ^{13}C NMR of the SdMBpyTMS ligand in chloroform-*d* (Figure 1a). The solid-state ^{13}C CP-MAS NMR spectra of SBA15(100)−SdMBpy (Figure 1b) possesses the same signals as the homogeneous form, but much broader because the SdMBpy ligands are now covalently immobilized and cannot rotate freely. The signal at 7.4 ppm corresponds to the $-CH_2Si-$ carbon, indicating the SdMBpy ligands were covalently anchored to the silica surface (verified by ^{29}Si MAS NMR). The weak bands centered at 192 and 105 ppm were determined to be the spinning sidebands of the 122 and 34 ppm signals, respectively. The immobilization of the CuBr/SdMBpyTMS complex onto silica was characterized by FT-Raman spectroscopy (Figure 2). Figure 2a shows FT-Raman spectra of SdMBpyTMS ligand. Table 3 summarizes the signals of interest for the SdMBpyTMS ligand.[55] Parts b and c of Figure 2 are the spectra for the immobilization on SBA-15(50) and SBA-15(100), respectively. The signals for the pyridyl rings and in-plane CH stretch were shifted to 1610 and 1554 and 1013 cm^{-1} (from 1607, 1560, and 996 cm^{-1}, respectively) which can be attributed to coordination of CuBr to the immobilized ligand. These signal shifts were consistent

Table 3. FT-Raman Spectroscopy of Silica-Supported CuBr/SdMBpy Catalysts

entry	material	ν(ar-CH)	ν(al-CH)	ν(pyridyl ring)	ν(in-plane CH)	ν(CS)
1	SdMBpyTMS	3056	2800−2900	1607, 1560	996	731
2	silica-CuBr/SdMBpy	3056	2800−2900	1610, 1554	1013	731

with those reported in the literature.[30,38,39] The slight peak shoulders remaining at 1607 cm^{-1} and more noticeably at 996 cm^{-1} may be attributed to uncoordinated ligands. Hence, it has been shown by ^{13}C CP-MAS NMR and FT-Raman that CuBr/SdMBpy complexes were covalently immobilized but more importantly that traces of uncoordinated ligands likely exist on the surface in addition to the immobilized mono- and bis-coordinated complexes.

Comparison of Immobilization Methods in the Literature. Covalent immobilization of tethered bpy ligands or complexes has been reported on polymer backbones[14,15,56] and inorganic supports[38,39,40,47] in the literature (note that incorporation of bpy complexes using methods other than formation of covalent linkages will not be discussed here because these methods will likely result in significant leaching of the complex from the solid).[28] Barnett,[40] Goncalves,[38,39] and Matyjaszewski[14,15] have utilized a multistep grafting approach to covalently immobilize (tether) bpy ligands to the surface. Although Barnett proposed the synthesis of an immobilizable bpy ligand to be covalently tethered to silica particles, the immobilizable ligand was never isolated prior to the addition of the solid support.[40]

To illustrate the difficulty associated with a multistep grafting approach, consider the work of Goncalves. Goncalves immobilized an oxomolybdenum/bpy complex on silica for the epoxidation of cyclooctene.[38,39] To tether or graft a bpy ligand to the surface, the dMBpy ligand was modified by first unsymmetrically deprotonating dMBpy with an LDA solution, followed by reacting the latter with 3-chloropropyl functionalities tethered to the surface. In the reported procedure, the silica surface was derivatized with 3-chloropropyltrimethoxysilane, resulting in 1.68 mmol of Cl/g of solid. After contacting the Li-dMBpy with the solid, the Cl composition decreased to 1.07 mmol of Cl/g of solid, corresponding to ca. 21% elimination of the Cl and addition of 0.29 mmol of Bpy/g of solid. Then the ligand was heterogeneously metalated with excess $MoO_2Cl_2(THF)_2$ to give the supported oxomolybdenum/bpy complex. By Mo microanalysis, an excess of Mo complex was incorporated into the solid (0.87 mmol of Mo/g of solid vs theoretical 0.29 mmol of Mo/g of solid), suggesting that in addition to coordinating to the bpy the Mo complex reacted with the bare silica surface. This ill-defined method for bpy complex immobilization poses several problems for ATRP applications. The unreacted Cl is undesired because halogen groups are potential initiating groups in ATRP (see reports of surface initiated ATRP in the literature[57−59]). In addition, the use of strong bases such as alkyl−lithium reagents is known to degrade silica materials; hence, the Li−Bpy can react with Si−O−Si and Si−OH bonds on the silica surface as well as with the intended chloropropyl groups.[60] Last, metal complexes bonded to the bare surface may possess drastically different reactivity than the tethered metal/ligand complexes. In a system where rapid initiation and good transport are essential, these problems are not amenable for well-controlled ATRP. Our attempts to immobilize CuBr/dMBpy complex on silica by this method resulted in a low ligand loading that was likely too limited for useful ATRP application.

Table 4. Polymerizations with Homogeneous Control Catalysts[a]

entry	catalyst	time (h)	% conv	$M_{n,th}$	$M_{n,exp}$	PDI
1	CuBr/SdMBpy	16	80	23 900	24 900	1.30
2	CuBr/p-SdMBpy	7	58	17 400	18 300	1.18
3	CuBr/p-SdMBpy[b]	6	94	28 200	30 200	1.22
4	CuBr/dMBpy/DPS	7	62	18 900	20 100	1.32

[a] Polymerization conditions: [MMA]/[ligand]/[Cu]/[BPN] = 300/2/1/1 in 50% by v/v MMA in toluene or diphenyl ether at 90 °C. [b] Diphenyl ether was the solvent.

Matyjaszewski reports bpy ligand/complexes immobilized on only polymer supports,[14,15] not silica. Like the Goncalves procedure, an asymmetrically deprotonated dMBpy ligand is reacted with a tethered Cl group (benzyl chloride) on the polymer bead support (PS8-dMBpy). The elimination of the Cl was reported to be quantitative (initially 1.14 mmol of Cl/g of resin; reacted 1.15 mmol of ligand/g of resin), indicating that the multistep grafting method is more useful for polymeric supports as there are limited side reactions.[14,15] However, it is later surmised that residual benzyl chloride sites can act as initiating sites that lead to polymerization off the support, coating the catalyst particle.[15] In addition, there are several other examples in the literature of tethering bpy ligands onto polymer backbones, and a recent review summarizes these.[56]

In this work, the immobilization of the ATRP complex was performed using the "preassembled complex approach".[30] The procedure involved constructing the CuBr/SdMBpyTMS (1:2 ratio to target bis-coordination) complex in solution prior to addition of the support. The advantage of the method is it reduces the potential interactions of bare CuBr with the surface. This is important because it was found that the surface silanols can act as a chemical ligand for the CuBr and the physisorbed CuBr cannot be removed readily, although a thorough wash with dichloromethane has been demonstrated to effectively remove free ligand and free metal complex that might be present in the materials.[30,31] The physisorbed, ligand-free CuBr was found to possess no activity for ATRP.[31] Using this technique, more well-defined immobilized complexes may be prepared, although the presence of small amounts of bare CuBr resulting from traces of preassembled complex decomposition upon immobilization cannot be ruled out, as nonaqueous solvent washes will not remove these species and the spectroscopic techniques utilized could not detect them.

Homogeneous Control Polymerizations of Methyl Methacrylate with CuBr/pSdMBpy. pSdMBpy was synthesized as a homogeneous analogue to the SdMBpyTMS immobilizable complex to determine whether the sulfur linkage affects the polymerization performance. Scheme 4 shows the different catalyst systems that were employed in control polymerizations. The results of these control experiments are summarized in Table 4. Figure 3 shows the first-order kinetic plots and the evolution of M_n and PDI with conversion for the homogeneous control experiments.

Polymerization with the typical CuBr/dMBpy catalyst in toluene solvent proceeded in well-controlled manner, reaching 80% conversion, with $M_{n,exp}$ agreeing well with

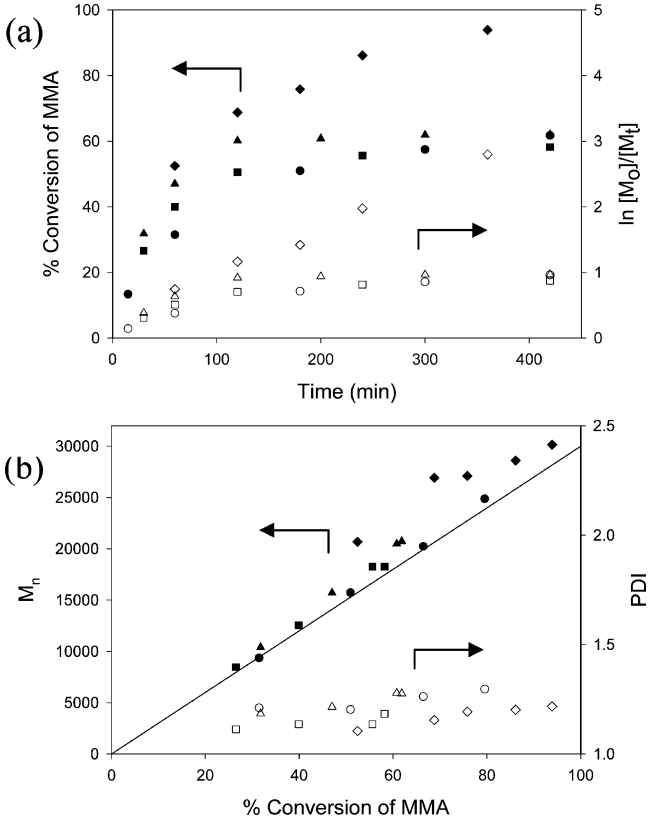

Figure 3. (a) Kinetic plots and (b) evolution of M_n and PDI vs % conversion of MMA plots for control experiments for homogeneous polymerizations with CuBr/dMBpy (●, ○), homogeneous polymerization with CuBr/dMBpy/DPS (▲, △), homogeneous polymerization with CuBr/pSdMBpy in toluene (■, □), and homogeneous polymerization with CuBr/pSdMBpy in diphenyl ether (♦, ◊). Theoretical M_n curve (—). Polymerization conditions: [MMA]/[Cu]/[BPN] = 300/1/1 in 50% by v/v MMA in toluene or diphenyl ether at 90 °C.

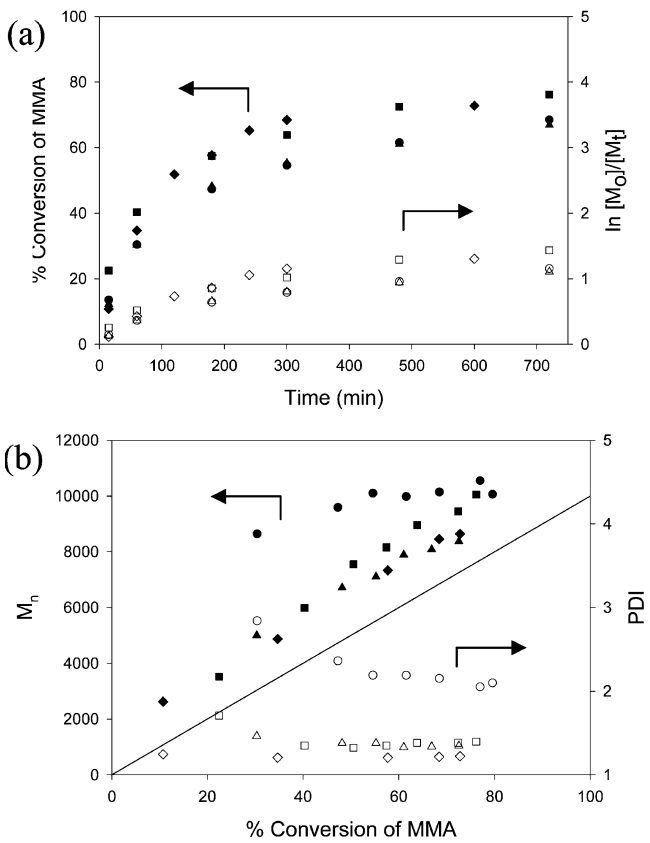

Figure 4. (a) Kinetic plots and (b) evolution of M_n and PDI vs % conversion of MMA plots for heterogeneous polymerizations with SBA15(100)-CuBr/SdMBpy (●, ○), CPG(240)-CuBr/SdMBpy (▲, △), Cab-O-Sil-CuBr/SdMBpy (■, □), and homogeneous polymerization with CuBr/dMBpy (♦, ◊). Theoretical M_n curve (—). Polymerization conditions: [MMA]/[Cu]/[BPN] = 100/1/1 in 25% by v/v MMA in toluene at 90 °C.

$M_{n,th}$ and with the resulting polymer having a narrow molecular weight distribution (PDI = 1.30, entry 1, Table 4). When using the homogeneous analogue of the immobilizable complex, CuBr/pSdMBpy (Scheme 4b), the conversion only reached 58% but was better controlled (PDI = 1.18, entry 2, Table 4). The lower conversion and improved PDI are likely due to better solubility due to the long flexible linker, causing more efficient chain deactivation.[3,5,61] When the solvent was switched from toluene to diphenyl ether, the polymerization with CuBr/pSdMBpy was much improved, owing to the increased solubility of the complex in diphenyl ether.[3,5,61,62] The conversion reached 94%, the $M_{n,exp}$ agreed well with $M_{n,th}$, and the molecular weight distribution was narrow (PDI = 1.22, entry 3, Table 4). The last control experiment involved using dipropyl sulfide (DPS) as an additive to see how the thioether affects the polymerization with CuBr/dMBpy (Scheme 4c). This polymerization proceeded similarly to CuBr/pSdMBpy polymerization in toluene (entry 4, Table 4), suggesting that the thioether does not inhibit the polymerization or affect the ability of the metal complexes to mediate the polymerization.

Results for Polymerization of Methyl Methacrylate with the Silica Immobilized CuBr/SdMBpy Catalysts. The silica immobilized CuBr/SdMBpy catalysts were tested for the polymerization of MMA at [MMA]/[Cu]/[BPN] = *X*/1/1 in *Y*% by v/v MMA in toluene at 90 °C (*X* = 300, *Y* = 50 or *X* = 100, *Y* = 25). Two different monomer/initiator ratios were chosen to determine how the target molecular weight affects the control of the polymerization. In addition, the role of silica support porosity was probed by utilizing four silica supports with substantially different pore structures. Figure 4 shows the first-order kinetic plots and the evolution of M_n and PDI with conversion for polymerizations with [MMA]/[BPN] = 100.

Table 5 summarizes the results of the polymerizations. Copper complexes supported on the SBA-15 supports were ineffective for controlling the polymerization. SBA15(50)-CuBr/SdMBpy polymerized with low conversion (44%) and very broad molecular weight distribution (PDI = 4.74). The larger pore size SBA15-(100)-CuBr/SdMBpy allowed for higher conversion (77%) and better control (2.11), but still uncontrolled when compared to well-behaved homogeneous ATRP catalysts (PDI ∼ 1.3 or better). However, CuBr/SdMBpy immobilized on CPG(240) and Cab-O-Sil were effective ATRP polymerization catalysts polymerizing with moderately high conversion (>70%) and good control (PDI < 1.35 or lower). Both catalysts produced a final polymer composition comparable to those produced by homogeneous catalysts CuBr/dMBpy and CuBr/pSdMBpy (entries 1 and 2, Table 4). The first-order kinetic plot shows evidence of some chain termination (Figure 4a), especially at higher conversions. The plots of M_n with conversion were linear (Figure 4b) and relatively parallel with the theoretical line, although molecular weights were always higher than predicted. This ob-

Table 5. MMA Polymerization with [MMA]/[BPN] = 100[a]

entry	catalyst	initial rate (mol/(L h))	time (h)	% conv	$M_{n,th}$	$M_{n,exp}$	PDI	R_{Cu} (ppm)
1	CuBr/dMBpy	0.86	10	74	7400	8 600	1.22	6840
2	SBA15(50)-CuBr/SdMBpy	0.76	24	44	4400	11 600	4.74	<10
3	SBA15(100)-CuBr/SdMBpy	1.08	24	77	7700	10 600	2.11	<10
4	CPG(240)-CuBr/SdMBpy	0.98	24	72	7200	8 400	1.35	<10
5	Cab-O-Sil-CuBr/SdMBpy	1.43	17	78	7800	13 000	1.29	<10

[a] Polymerization conditions: [MMA]/[Cu]/[BPN] = 100/1/1 in 25% by v/v MMA in toluene at 90 °C.

Table 6. MMA Polymerization with [MMA]/[BPN] = 300[a]

entry	catalyst	initial rate (mol/(L h))	time (h)	% conv	$M_{n,th}$	$M_{n,exp}$	PDI	R_{Cu} (ppm)
1	CuBr/dMBpy	2.25	16	79	23 700	24 900	1.30	1324
2	SBA15(100)-CuBr/SdMBpy	2.54	24	79	23 800	31 200	1.81	48
3	CPG(240)-CuBr/SdMBpy	1.76	24	70	21 000	25 700	1.38	168
4	Cab-O-Sil-CuBr/SdMBpy	5.62	24	76	22 800	27 700	1.52	<10

[a] Polymerization conditions: [MMA]/[Cu]/[BPN] = 300/1/1 in 50% by v/v MMA in toluene at 90 °C.

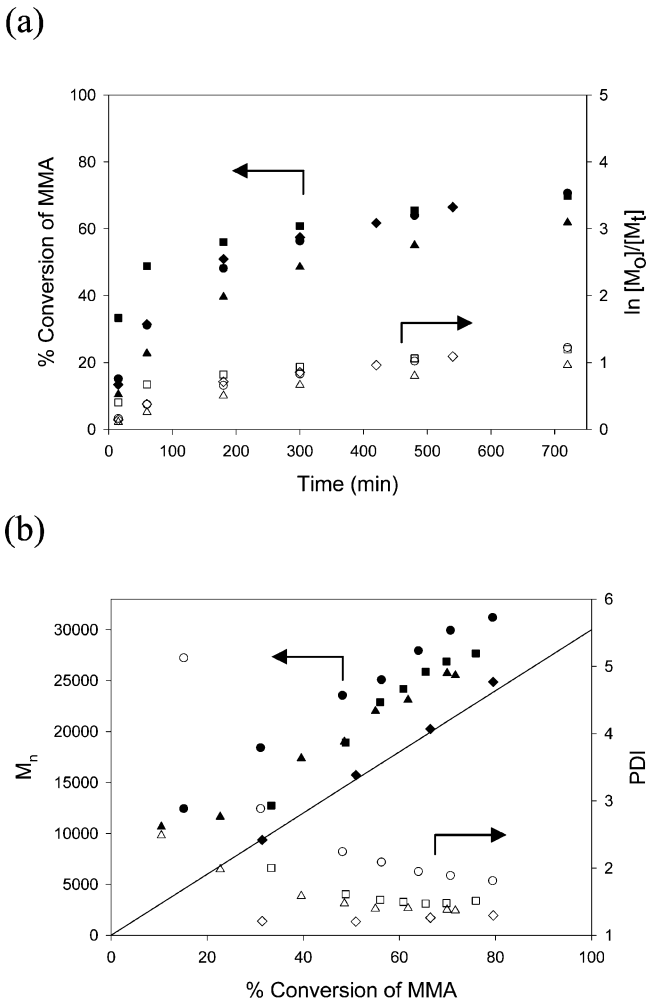

Figure 5. (a) Kinetic plots and (b) evolution of M_n and PDI vs % conversion of MMA plots for heterogeneous polymerizations with SBA15(100)-CuBr/SdMBpy (●, ○), CPG(240)-CuBr/SdMBpy (▲, △), Cab-O-Sil-CuBr/SdMBpy (■, □), and homogeneous polymerization with CuBr/dMBpy (♦, ◇). Theoretical M_n curve (—). Polymerization conditions: [MMA]/[Cu]/[BPN] = 300/1/1 in 25% by v/v MMA in toluene at 90 °C.

servation is common to supported ATRP catalysts and may result from poor deactivation of the growing chain at the outset of the polymerization.[13−15] The residual copper content, R_{Cu}, was less than 10 ppm in all the polymers analyzed (10 ppm was the detection limit of the analyses).

Figure 5 shows the first-order kinetic plots and the evolution of M_n and PDI with conversion for polymerizations with [MMA]/[BPN] = 300. Table 6 summarizes the polymerization results. Polymerization with SBA15-(50)-CuBr/SdMBpy catalyst was not performed because of the poor performance for polymerization where [MMA]/[BPN] = 100. Polymerization with SBA15(100)-CuBr/SdMBpy was still ineffective as evidenced by the broad molecular weight distribution (PDI = 1.81). Again, polymerizations with CuBr/SdMBpy immobilized on CPG(240) and Cab-O-Sil supports (entries 3 and 4, Table 6) were well controlled (CPG(240) with better control).

The conversion and molecular weight distributions were comparable to homogeneous polymerization with CuBr/dMBpy and CuBr/pSdMBpy. The first-order kinetic plots show evidence of some chain termination at high conversions (Figure 5a). The plots of M_n with conversion were linear (Figure 5b) and parallel with the theoretical line, although molecular weights were higher than predicted. The molecular weight distributions for both cases were slightly higher for polymerizations at the lower [MMA]/[BPN] ratio. This was attributed to the increased viscosity of the solutions, causing less efficient transport in solution. The R_{Cu} were no greater than 168 ppm in the polymers when catalyst recovery was done by sedimentation. However, when centrifugation was used to recover Cab-O-Sil-CuBr/SdMBPy, the R_{Cu} was less than 10 ppm. This observation may indicate that the higher Cu content in the final polymer (Table 6, entries 2 and 3) is due to entrapped silica catalyst. Figure 6 shows an image of polymers prepared homogeneously with CuBr/dMBpy and heterogeneously with silica-CuBr/SdMBpy catalysts. The polymerization with all the immobilized silica-CuBr/SdMBpy catalysts afforded white polymers with no green color to them, giving visual confirmation of the supported catalysts ability to sequester the copper species with limited leaching.

Although the undetectable Cu content in the final polymers and narrow PDI ([MMA]/[BPN] = 100) give hope to the notion that a completely recoverable silica-supported ATRP catalyst may be in hand, there is not sufficient evidence to draw this conclusion. In fact, when three of the catalysts used in this work were analyzed for Cu content after the polymerization, it was apparent that some Cu leaching had occurred from the porous catalysts [SBA-15(100): Cu/Si = 0.135 before and Cu/

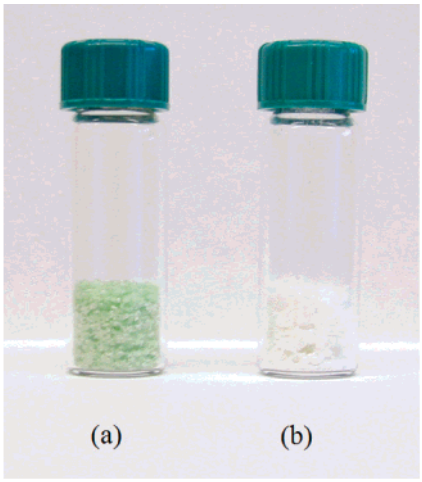

Figure 6. Polymers produced with (a) homogeneous polymerization with CuBr/dMBpy and (b) heterogeneous polymerization with silica-supported CuBr/SdMBpy catalysts.

Si = 0.105 after; CPG(240): Cu/Si = 0.076 before and Cu/Si = 0.065 after; Cab-O-Sil: Cu/Si = 0.069 before and Cu/Si = 0.064 after]. Furthermore, it is noted that when Matyjaszewski utilizes the homogeneous deactivator in conjunction with polymer supported CuBr/Bpy catalysts, excellent control can be obtained with soluble Cu concentrations as low as 15 ppm.[15] With a 10 ppm detection limit in EA, one cannot rule out residual homogeneous copper concentrations of this magnitude (∼10 ppm). Indeed, there is no evidence in the open literature that good polymerization control can be achieved with no complex leaching. A small concentration of leached or homogeneous complex may in fact be a prerequisite for good polymerization control with supported systems. This hypothesis fits with many prominent literature reports to date, for example refs 15 and 31.

Effect of Silica Support Structure. Of the three silica supports evaluated, CPG(240) and Cab-O-Sil EH5 were the most effective, with CPG(240) being more effective at higher [MMA]/[BPN] ratio. Cab-O-Sil EH5 is a commercially available fumed silica with a very small primary particle size, making it moderately soluble in hot toluene. Furthermore, it has no measurable porosity, meaning that all of its surface area is external. CPG(240) is also a commercially available porous silica with large polydisperse pore size and interconnecting pore network. In contrast, SBA-15 is a mesoporous silica material with straight mesopores in a hexagonal array.[34,35] Although the mesopores are connected by small micropores,[63] these micropores can be considered unimportant for the diffusion of relatively large species like polymer chains. Hence, in these polymerizations, each pore in the SBA-15 is essentially an isolated reaction environment with only a single entrance point and exit point at each end. These very different porosities of the supports would be expected to play a role in the effectiveness of the polymerizations. Indeed, porosity does play a key role because the accessibility of the catalyst complex can be limited by the size of the pore and growing polymer.

The fact that CPG(240) and Cab-O-Sil supported catalysts give the best control over the polymerization points to the paramount importance of access of the growing polymer chain to the metal complexes, as previously reported in the literature.[13−15,30,31] It is important that the growing polymer chain can access the $CuBr_2$ complexes relatively easily and return to their dormant state. The ease of this deactivation process is critical to having a controlled polymerization. When considering the porous SBA-15 catalysts, we observe that the polymerizations are generally less controlled, with the restricted mobility of the growing chains within the pores affecting the polymerization process. In the case of CPG(240), the larger interconnecting pore network facilitates transport and ultimately leads to better control because the pores are not isolated like SBA-15. The length of the flexible linker also contributes to improved control because it may allow the CuBr/SdMBpy complex to be solvated even when it is immobilized to a support. Indeed, Zhu showed that an optimized length for the support surface linkage leads to polymerizations with better control.[26] On the other hand, Cab-O-Sil is a nanosized and nonporous solid with less diffusion limitations compared to the other three supports. In addition, because of its small primary particle size, Cab-O-Sil is more miscible in toluene at the polymerization temperature. In this work, the best polymerization control over the polymerization was observed with Cab-O-Sil-CuBr/SdMBpy catalyst at [MMA]/[BPN] = 100. Slightly less control was observed at the higher ratio because the polymerization mixture started to gel (viscosity increased) as conversion increased. These are among the best controlled polymerizations reported on silica without using a deactivator, with PDIs akin to those reported by Zhu.[26]

The initial rates for the polymerizations increased as follows for the supports: SBA-15(50) < CPG(240)∼SBA-15(100) < Cab-O-Sil. These results were inline with previous work on CuBr/PMI catalysts immobilized on different supports.[31] Higher initial rates were observed as pore size increases, with the highest over the nonporous catalyst. These observations were consistent with entrapment of some growing polymer chains within the mesopores of the SBA-15 supports, resulting in slower polymerization rates.

Application of a Soluble Deactivator in Silica-Supported Systems. Polymerizations with bpy catalysts immobilized by a multistep grafting method on traditional polymeric supports have been shown to be ineffective for mediating well-controlled ATRP, for example reaching only moderate conversions (59%), with $M_{n,exp}$ greatly disagreeing with $M_{n,th}$ (71 200 vs 17 100) and with a broad molecular weight distribution (PDI = 2.26).[14,15] This limited performance in controlling the polymerization has been attributed to an inefficient deactivation of the growing polymer chain resulting in uncontrolled propagation. To improve the deactivation process, a soluble deactivator complex, $CuBr_2$/Me_6-TREN, was introduced with positive results.[14,15] With the deactivator, the polymerization reached 96% conversion, $M_{n,exp}$ agreed well with $M_{n,th}$, and the molecular weight distribution was narrow (PDI = 1.29). This result clearly suggests the deactivation process was the cause of the poor catalysts performance. Use of a soluble deactivator is also reported with silica-supported catalysts, although the available data are more limited.[15]

The soluble deactivator method may not be as efficient when silica supports are used due to strong interactions between the silica surface and the homogeneous complex as discussed below. Matyjaszewski's $CuBr_2$/Me_6TREN deactivator complex was tested with the silica-CuBr/SdMBpy catalysts to determine whether the

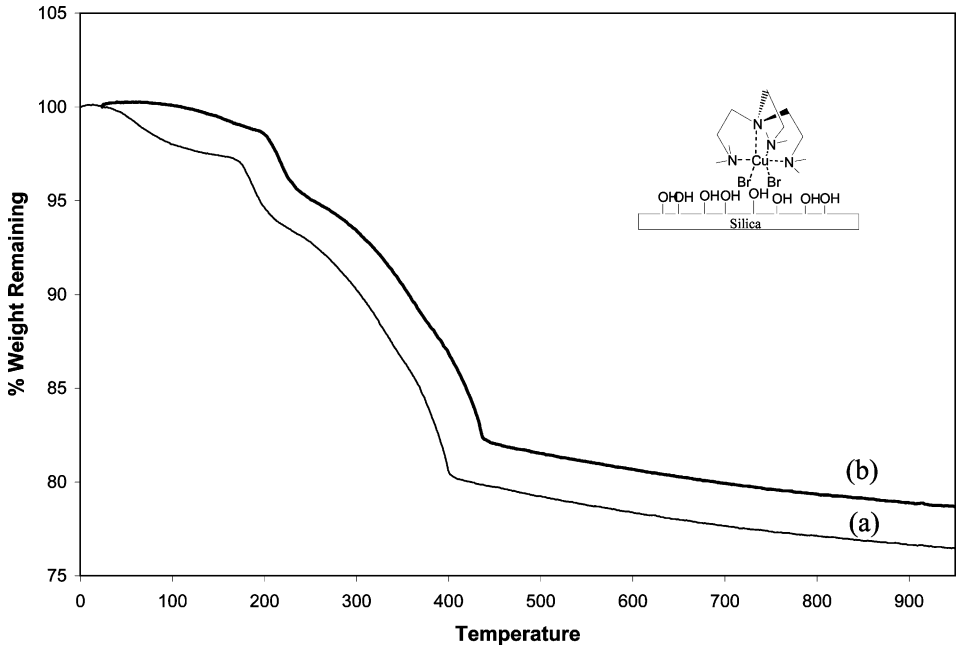

Figure 7. Thermogravimetric analysis curves for control experiment with $CuBr_2/Me_6TREN$ on CPG(240): (a) $CuBr_2/Me_6TREN$/CPG(240) washed with toluene and (b) $CuBr_2/Me_6TREN$/CPG(240) washed with dichloromethane and THF.

conversion and polydispersity can be improved upon. When 5 mol % $CuBr_2/Me_6TREN$ (relative to immobilized copper) was added to the polymerization mixture with CPG(240)-CuBr/SdMBpy ([MMA]/[BPN] = 300), no improvement in the PDI was observed (conversion 73% and PDI = 1.51), although the $M_{n,exp}$ = 22 900 agreed better with $M_{n,th}$ = 21 900. It was speculated that the deactivator complex strongly adsorbed to the support surface similarly to Zhu's physisorbed CuBr/HMTETA ATRP system (aliphatic amines are known to adsorb strongly to silica).[22,23] The deactivator complex would now act as an immobilized complex and not its intended function, as a "shuttling agent" for the halogen. Two control experiments were undertaken to verify our assumption. First, the $CuBr_2/Me_6TREN$ complex (20 wt %) was contacted with pristine CPG(240) silica (80 wt %) in dry toluene (polymerization solvent) and stirred for 1 h. The solid was then recovered and washed in the glovebox with copious amount of toluene and vacuum-dried. The same solid was then washed with copious amount of dry dichloromethane and THF and vacuum-dried. Figure 7 shows both thermogravimetric weight loss curves for $CuBr_2/Me_6TREN$/CPG(240) washed with toluene (a) and $CuBr_2/Me_6TREN$/CPG(240) washed with dichloromethane and THF (b) samples. The toluene wash was not able to remove any of the $CuBr_2/Me_6$-TREN, and the dichloromethane and THF wash was only able to remove a small amount. To see whether the deactivator complex was interacting with the surface silanols, the same control experiment described above was performed with CPG(240) that was previously contacted with HMDS to remove the accessible surface silanols ("capped" CPG(240)). Figure 8 shows the thermogravimetric weight loss curves for bare capped CPG-(240) (a), $CuBr_2/Me_6TREN$/capped CPG(240) washed with toluene (b), and $CuBr_2/Me_6TREN$/capped CPG(240) washed with dichloromethane and THF (c). The toluene was unable to remove the complex, although the dichloromethane and THF wash was able to remove much of the adsorbed species. Nonetheless, some chemisorbed complex remained on the surface. These results indicate that the deactivator complex interacts with the silica surface, and the nonpolar toluene solvent likely partitions the highly polar complex to the polar silica even when the surface silanols were removed. As a consequence, when using silica as the support, the deactivator complex is found to be ineffective for improving the deactivation process under the conditions reported here. Fortunately, with the current catalyst design, the deactivator was not needed because the CPG(240)- and Cab-O-Sil-CuBr/SdMBpy catalysts polymerize with excellent control and reasonable conversions in the absence of any added homogeneous agent (although some homogeneous species may exist due to leaching).

Regeneration of the Immobilized Silica-CuBr/SdMBpy Catalysts. In previous studies done by Matyjaszewski[15] and Zhu,[25] the immobilized CuBr/ligand has been regenerated back to the initial Cu(I) oxidation state for catalyst reuse. Without the regeneration process, the catalyst exhibited low activity and poor control because of the buildup of a high concentration of Cu(II) due to termination reactions. In addition, there have also been reports of ligand loss after each reuse (second reuse, decrease = 39%; third reuse, decrease = 58%).[15] In our work with immobilized silica-CuBr/PMI catalysts, the catalysts did not require regeneration and possessed reasonable activity and improved control up to the sixth reuse at the same [Cu]/[Initiator] of the first use. This has been attributed to the presence of substantial leached copper species in the $CuBr/PMI/SiO_2$ system.[31] Unfortunately, polymerizations with recycled Cab-O-Sil-CuBr/SdMBpy catalyst without regeneration proceeded only very slowly ([MMA]/[BPN] = 100; first use, conversion = 78% and PDI = 1.29 in 17 h; second use, conversion = 45% and PDI = 1.24 in 89 h), perhaps due to the fact that there is very limited or no leaching in this system. A slight improvement in molecular weight distribution when using recycled catalyst was observed, similar to immobilized CuBr/PMI systems.[31] The improvement was speculated to be due to the presence of Cu(II) at the beginning of the polymerization which slowed down the initial uncontrolled propagation commonly observed with immobilized ATRP catalysts. The recovered silica-CuBr/SdMBpy catalysts possessed a

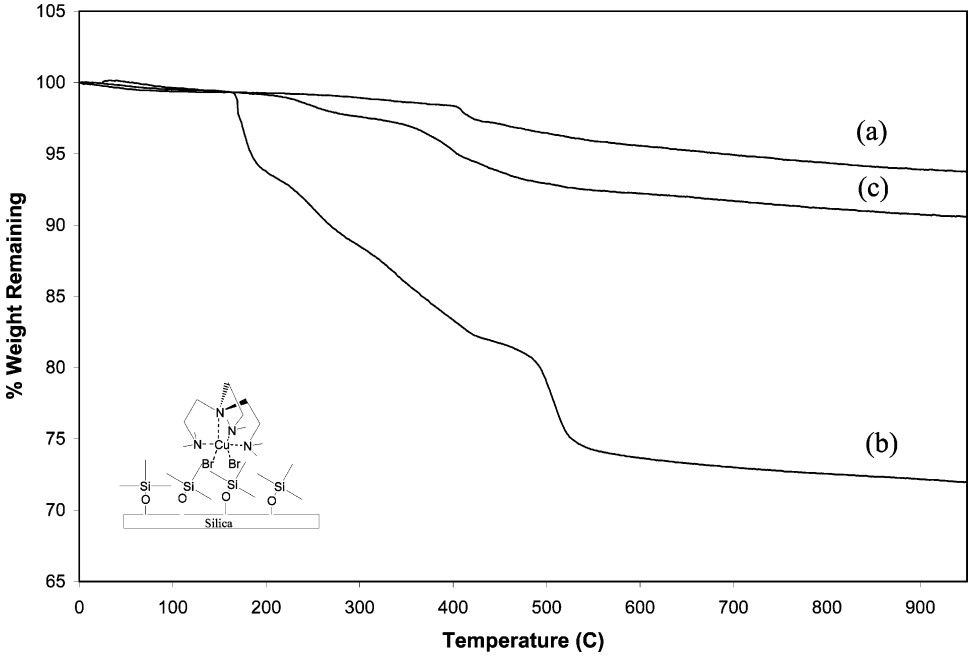

Figure 8. Thermogravimetric analysis curves for control experiment with $CuBr_2/Me_6TREN$ on capped CPG(240): (a) bare capped CPG(240), (b) $CuBr_2/Me_6TREN$/capped CPG(240) washed with toluene, and (c) $CuBr_2/Me_6TREN$/capped CPG(240) washed with dichloromethane and THF.

Table 7. Polymerization with Recycled Catalysts[a]

entry	catalyst	[M]/[I]	time (h)	% conv	$M_{n,th}$	$M_{n,exp}$	PDI
1	Cab-O-Sil-CuB/SdMBpy-1	100	17	78	7 800	13 000	1.29
2	Cab-O-Sil-CuB/SdMBpy-2[b]	100	89	45	4 500	5 700	1.24
3	Cab-O-Sil-CuB/SdMBpy-3[c]	100	24	54	5 400	7 500	1.32
4	Cab-O-Sil-CuB/SdMBpy-4[c]	100	48	65	6 500	7 600	1.23
5	CPG(240)-CuBr/SdMBpy-1	300	24	70	21 000	25 700	1.38
6	CPG(240)-CuBr/SdMBpy-2[b]	300	48	60	18 100	17 100	1.41
7	CPG(240)-CuBr/SdMBpy-3[c]	300	72	50	15 000	15 600	1.34

[a] Polymerization conditions: [MMA]/[BPN]/[Cu] = X/1 in Y% by v/v MMA in toluene at 90 °C ($X = 100$, $Y = 25$; $X = 300$, $Y = 50$). [b] Polymerization without catalyst regeneration. [c] Polymerization with catalyst regenerated with AIBN.

green color due to the high concentration of Cu(II) complexes immobilized. Therefore, it seemed essential to reduce the immobilized Cu(II) complex back to the Cu(I) oxidation state to have catalysts with reasonable activity, as others have previously reported.[15,25]

Typical regeneration procedures involve stirring the used catalyst with zerovalent copper powder or wire,[15,25] allowing the Cu(0) to reduce the Cu(II) back to Cu(I). Application of the $CuBr_2/Me_6TREN$ complex as a "halogen-delivery messenger" in conjunction with copper wire was found to be a useful method of catalyst regeneration.[15] The Cu(0) wire reduces the $CuBr_2/Me_6TREN$ to $CuBr/Me_6TREN$. Since the $CuBr/Me_6TREN$ complex prefers to be in the Cu(II) oxidation state, it then reduces the immobilized $CuBr_2$/dMBpy catalysts to Cu(I) state and is itself reconverted to $CuBr_2/Me_6TREN$ complex. Unfortunately, as demonstrated above, $CuBr_2/Me_6TREN$ adsorbs strongly to silica and can be ineffective for the halogen exchange process using the system reported here. Therefore, another regeneration technique needed to be developed so that the catalyst could be recycled.

To this end, we have developed a simple regeneration process involving a process akin to reverse ATRP.[64,65] In reverse ATRP, the oxidation state of the copper complex is initially Cu(II), and the initiating group does not possess a halogen. A polymerization is initiated by conventional means, and the high oxidation state metal complex serves to deactivate the growing chains. Promoting reverse ATRP with the used catalyst was probed as a methodology of regenerating/recycling the catalyst; however, it produced poor polymerization results ([MMA]/[BPN] = 300; conversion = 93%, $M_{n,exp} = 19\,000$, and PDI = 1.91) with the used CPG(240)-$CuBr/CuBr_2$/SdMBpy catalyst. Therefore, a regeneration process was developed that utilized AIBN as a catalyst treatment but without addition of monomer. When 1 equiv of AIBN (to immobilized Cu) was added to the used catalyst in toluene and stirred at 90 °C for 15 min, the solid turned from a dark green to dark red color. The color change of the solid indicated that a higher concentration of the immobilized copper exists in the Cu(I) oxidation state. The solid catalysts were recovered by filtration in the nitrogen glovebox, washed with copious amount of toluene and dichloromethane (to remove AIBN-derived species), vacuum-dried overnight, and stored in a nitrogen glovebox until further use. Note that when the regeneration process was carried out for a longer time, the solid turned dark red initially, but eventually became dark green color. Therefore, the regeneration time should remain short, but the exact time has not yet been optimized to achieve the highest concentration of immobilized Cu(I) complexes (15 min was the time used in this work).

Catalyst Recycling with AIBN Regenerated Catalysts. Catalysts regenerated with AIBN were recycled, and the results are summarized in Table 7. The polymerization conditions used the same initial copper loading

to determine the appropriate amount of monomer, initiator, and solvent to be added. Polymerizations with nonregenerated Cab-O-Sil-CuBr/SdMBpy proceed slower than the initial use ([MMA]/[BPN] = 100: first use, conversion = 78% in 17 h; second use, conversion = 45% in 89 h). However, when the catalyst was regenerated, the polymerization proceed faster than without the regeneration, but still slower than the first use (third use, conversion = 54% in 24 h). In both cases, the molecular weight distributions were comparable to the first use (PDI = 1.29, 1.24, and 1.31 for first, second, and third use, respectively). $M_{n,exp}$ was always determined to be higher than the $M_{n,th}$. The catalyst was then regenerated a second time, and the catalysts was reused for a fourth time. This time the polymerization was allowed to run for 48 h, achieving 65% conversion and PDI = 1.23. The lower conversion was attributed to the presence of immobilized Cu(II) that was not regenerated. Results for polymerizations with AIBN-regenerated CPG(240)-CuBr/SdMBpy catalyst at the higher [MMA]/[BPN] ratio were similar to that of Cab-O-Sil-CuBr/SdMBpy described above. The activities were lower and the molecular weight distributions were comparable to the first use, but the $M_{n,exp}$ agreed better with the $M_{n,th}$. The lower conversions exhibited here could potentially be due to pore clogging, in addition to the presence of immobilized Cu(II). As noted above, the immobilized catalysts reported here can be recycled by regeneration with AIBN. This regeneration technique is a useful addition to those previously described in the literature because no additional metal is added to the system.

Summary

A well-defined, immobilizable SdMBpyTMS ligand was synthesized and coordinated with CuBr and the CuBr/SdMBpyTMS ATRP complex was covalently immobilized on four different silica supports in one step. Characterization by a battery of techniques (^{13}C CP-MAS NMR, ^{29}Si CP-MAS NMR, FT-Raman spectroscopy, and elemental and thermogravimetric analyses) demonstrated that direct immobilization of the CuBr/SdMBpy complex was successful and the surface species consisted of immobilized mono- and bis-copper coordinated bpys, immobilized uncoordinated bpys, and possibly small amounts of physisorbed copper. These catalysts were tested for the controlled polymerization of methyl methacrylate. SBA-15 type supports were ineffective catalysts because effective mass transport (and hence efficient deactivation) was inhibited by the pore size and isolated structure of the pore network. However, when using a support with a random network of larger pores (CPG(240)) and a nonporous and nanosized support (Cab-O-Sil EH5), controlled polymerizations were readily obtained. These catalysts allowed polymerizations to achieve reasonably high conversions with narrow molecular weight distributions. The polymers recovered possessed very low copper content in all cases, with most catalysts giving undetectable amount of Cu, implying that the catalysts did not leach to a significant extent. For the system described here, the conversion could not be improved by using Matyjaszewski's $CuBr_2$/Me_6TREN complex (immobilized/soluble hybrid catalyst) because the soluble deactivator species adsorbed to the silica support strongly, therefore restricting its ability to act as a "shuttling agent". In addition, the $CuBr_2$/Me_6TREN complex could not be used as a "halogen-delivery messenger" as described in published regeneration procedures using Cu(0) as a reductant.[15] A new regeneration procedure was developed using AIBN to reduce the immobilized Cu(II) complex. Regeneration by this new procedure eliminates addition of new copper metal into the system, and the performance of the regenerated catalysts is on par with the first use. Thus, a new, recyclable silica-supported catalyst system that results in well-controlled polymerizations has been described along with a unique methodology for catalyst regeneration.

Acknowledgment. The National Science Foundation is gratefully acknowledged for the partial support of this work (CTS-0210460). C.W.J. thanks the Shell Oil Company Foundation and Oak Ridge Associated Universities for partial support of this work through a Faculty Career Initiation Award and a Ralph Powe Junior Faculty Award, respectively. We thank Dr. Angus Wilkinson for the use of the X-ray diffractometer and Dr. Johannes Liesen for advice with solid-state NMR experiments.

References and Notes

(1) Wang, J.; Matyjaszewski, K. *J. Am. Chem. Soc.* **1995**, *117*, 5614−5615.
(2) Wang, J.; Matyjaszewski, K. *Macromolecules* **1995**, *28*, 7572−7573.
(3) Wang, J.; Matyjaszewski, K. *Macromolecules* **1995**, *28*, 7901−7910.
(4) Kato, M.; Kamigaito, M.; Sawamoto, M.; Higashimura, T. *Macromolecules* **1995**, *28*, 1721−1723.
(5) Wang, J.; Matyjaszewski, K. *Chem. Rev.* **2001**, *101*, 2921−2990.
(6) Matyjaszewski, K.; Pintauer, T.; Gaynor, S. *Macromolecules* **2000**, *33*, 1476−1478.
(7) Haddleton, D. M.; Jackson, S. G.; Bon, S. A. F. *J. Am. Chem. Soc.* **2000**, *122*, 1542−1543.
(8) Angot, S.; Ayres, N.; Bon, S. A. F.; Haddleton, D. M. *Macromolecules* **2001**, *34*, 768−774.
(9) Biedron, T.; Kubisa, P. *Macromol. Rapid Commun.* **2001**, *22*, 1237−1242.
(10) Sarbu, T.; Matyjaszewski, K. *Macromol. Chem. Phys.* **2001**, *202*, 3379−3391.
(11) Carmichael, A. J.; Haddleton, D. M.; Bon, S. A. F.; Seddon, K. R. *Chem. Commun.* **2000**, 1237−1238.
(12) Honigfort, M. E.; Brittain, W. J.; Bosanac, T.; Wilcos, C. S. *Macromolecules* **2002**, *35*, 4849.
(13) Kickelbick, G.; Paik, H. J.; Matyjaszewski, K. *Macromolecules* **1999**, *32*, 2941−2947.
(14) Hong, S. C.; Paik, H. J.; Matyjaszewski, K. *Macromolecules* **2001**, *34*, 5099−5102.
(15) Hong, S. C.; Matyjaszewski, K. *Macromolecules* **2002**, *35*, 7592−7605.
(16) Hong, S. C.; Neugebauer, D.; Inoue, Y.; Lutz, J. F.; Matyjaszewski, K. *Macromolecules* **2003**, *36*, 27−35.
(17) Hong, S. C.; Lutz, J. F.; Inoue, Y.; Strissel, C.; Nuyken, O.; Matyjaszewski, K. *Macromolecules* **2003**, *36*, 1075−1082.
(18) Haddleton, D. M.; Kukulj, D.; Radigue, A. P. *Chem. Commun.* **1999**, 99−100.
(19) Haddleton, D. M.; Duncalf, D. J. Kukulj, D.; Radigue, A. P. *Macromolecules* **1999**, *32*, 4769−4775.
(20) Liou, S.; Rademacher, J. T.; Malaba, D.; Pallack, M. E.; Brittain, W. J. *Macromolecules* **2000**, *33*, 4295−4296.
(21) Hognifort, M. E.; Brittain, W. J. *Macromolecules* **2003**, *36*, 3111−3114.
(22) Shen, Y.; Zhu, S.; Zeng, F.; Pelton, R. *Macromol. Chem. Phys.* **2001**, *201*, 1387−1394.
(23) Shen, Y.; Zhu, S.; Zeng, F.; Pelton, R. *Macromolecules* **2000**, *33*, 5427−5431.
(24) Shen, Y.; Zhu, S.; Pelton, R. *Macromolecules* **2001**, *34*, 3182−3185.
(25) Shen, Y.; Zhu, S.; Zeng, F.; Pelton, R. *J. Polym. Sci., Polym. Chem.* **2001**, *39*, 1051−1059.
(26) Shen, Y.; Zhu, S.; Pelton, R. *Macromolecules* **2001**, *34*, 5812−5818.
(27) Shen, Y.; Zhu, S. *Macromolecules* **2001**, *34*, 8603−8609.

(28) Shen, Y.; Zhu, S.; Pelton, R. *Macromol. Rapid Commun.* **2000**, *21*, 956−959.
(29) Opstal, T.; Melis, K.; Verpoort, F. *Catal. Lett.* **2001**, *74*, 155−159.
(30) Nguyen, J. V.; Jones, C. W. Part 1, *J. Polym. Sci., Polym. Chem.*, in press.
(31) Nguyen, J. V.; Jones, C. W. Part 2, *J. Polym. Sci., Polym. Chem.*, in press.
(32) Pangborn, A. M.; Giardello, M. A.; Grubbs, R. H.; Rosen, R. K.; Timmers, F. J. *Organometallics* **1996**, *15*, 1518−1520.
(33) Ciampolini, M.; Nard, N. *Inorg. Chem.* **1966**, *5*, 41.
(34) Zhao, D.; Feng, J.; Huo, Q.; Melosh, N.; Frederickson, G. H.; Chmelka, B. F.; Stucky, G. D. *Science* **1998**, *279*, 548−552.
(35) Zhao, D.; Huo, Q.; Feng, J.; Chmelka, B. F.; Stucky, G. D. *J. Am. Chem. Soc.* **1998**, *120*, 6024−6036.
(36) Griggs, C. G.; Smith, D. J. H. *J. Chem. Soc., Perkin Trans.* **1982**, 3041−3053.
(37) Kruk, M.; Jaroniec, M. *Chem. Mater.* **2000**, *12*, 1961−1968.
(38) Nunes, C. D.; Valente, A. A.; Pillinger, M.; Fernandes, A. C.; Romao, C. C.; Rocha, J.; Goncalves, I. S. *J. Mater. Chem.* **2002**, *12*, 1735−1742.
(39) Nunes, C. D.; Pillinger, M.; Valente, A. A.; Goncalves, I. S.; Rocha, J.; Ferreira, P.; Kuhn, F. E. *Eur. J. Inorg. Chem.* **2002**, 1100−1107.
(40) Barnett, N. W.; Bos, R.; Brand, H.; Jones, P.; Lim, K. F.; Purcell, S. D.; Russel, R. A. *Analyst* **2002**, *127*, 455−458.
(41) Geneste, F.; Moinet, C.; Jezequel, G. *New J. Chem.* **2002**, *26*, 1539−1541.
(42) Maillet, C.; Janvier, P.; Pipelier, M.; Praveen, T.; Andres, Y.; Bujoli, B. *Chem. Mater.* **2001**, *13*, 2879−2884.
(43) Maillet, C.; Janvier, P.; Pipelier, M.; Bertrand, M. J.; Praveen, T.; Bujoli, B. *Eur. J. Org. Chem.* **2002**, 1685−1689.
(44) Mongey, K. F.; Vos, J. G.; MacCraith, B. D.; McDonagh, C. M.; Coates, C.; McGarvey, J. J. *J. Mater. Chem.* **1997**, *7*, 1473−1479.
(45) Ogawa, M.; Nakamura, T.; Mori, J. I.; Kuroda, K. *Microporous Mesoporous Mater.* **2000**, *48*, 159−164.
(46) Collinson, M. M.; Novak, B.; Skylar, M.; Taussig, J. S. *Anal. Chem.* **2000**, *72*, 2914−2918.
(47) Gosh, P. K.; Spiro, T. G. *J. Am. Chem. Soc.* **1980**, *102*, 5543−5549.
(48) Cheng, K. A.; Lin, W. Y.; Li, S. G.; Che, C. M.; Pang, W. Q. *New J. Chem.* **1999**, *23*, 733−737.
(49) Li, H. R.; Lin, J.; Zhang, H. J.; Li, H. C.; Fu, L. S.; Meng, Q. G. *Chem. Commun.* **2001**, 1212−1213.
(50) Odobel, F.; Bujoli, B.; Massiot, D. *Chem. Mater.* **2001**, *13*, 163−173.
(51) Odobel, F.; Massiot, D.; Harrison, B. S.; Schanze, K. S. *Langmuir* **2003**, *19*, 30−39.
(52) Sato, Y.; Kagotani, M.; Souma, Y. *J. Mol. Catal. A.* **2000**, *151*, 79−85.
(53) Smith, M. B.; March, J. March's *Advanced Organic Synthesis: Reactions, Mechanism, and Structure*, 5th ed; John Wiley & Sons: New York, 2001; p 998.
(54) Sindorf, D. W.; Maciel, G. E. *J. Am. Chem. Soc.* **1983**, *105*, 3767−3776.
(55) Baranska, H.; Labudzinska, A.; Terpinski, J. *Laser Raman Spectrometry*; John Wiley and Sons: New York, 1987.
(56) Kaes, C.; Katz, A.; Hosseini, M. W. *Chem. Rev.* **2000**, *100*, 3553−3590.
(57) Zheng, G.; Stoever, H. D. H. *Macromolecules* **2002**, *35*, 6828−6834.
(58) Tsujii, Y.; Ejaz, M.; Yamamoto, S.; Fukuda, T.; Shigeto, K.; Mibu, K.; Shinjo, T. *Polymer* **2002**, *43*, 3837−3841.
(59) Jeyaprakash, J. D.; Samuel, S.; Dhamodharan, R.; Ruhe, J. *Macromol. Rapid Commun.* **2002**, *23*, 277−281.
(60) Tao, T.; Maciel, G. E. *J. Am. Chem. Soc.* **2000**, *122*, 3118−3126.
(61) Wang, J. L.; Grimaud, T.; Matyjaszewski, K. *Macromolecules* **1997**, *30*, 6507−6512.
(62) de la Fuente, J. L.; Fernandez-Sanz, M.; Fernandez-Garcia, M.; Madruga, E. L. *Macromol. Chem. Phys.* **2001**, *202*, 2565−2571.
(63) Imperor-Clerc, M.; Davidson, P.; Davidson, A. *J. Am. Chem. Soc.* **2000**, *48*, 11925−11933.
(64) Matyjaszewski, K.; Woodworth, B. E. *Macromolecules* **1998**, *31*, 4718−4723.
(65) Xia, J.; Matyjaszewski, K. *Macromolecules* **1999**, *32*, 5199−5202.

MA0354391